TARGET SELECTION FOR SETI. II. TYCHO-2 DWARFS, OLD OPEN CLUSTERS, AND THE NEAREST 100 STARS

Margaret C. Turnbull

University of Arizona, Steward Observatory, 933 North Cherry Avenue, Tucson, AZ 85721; turnbull@as.arizona.edu

AND

Jill C. Tarter

SETI Institute, 2035 Landings Drive, Mountain View, CA 94043; tarter@seti.org

ABSTRACT

We present the full target list and prioritization algorithm developed for use by the microwave search for technological signals at the SETI Institute. We have included the Catalog of Nearby Habitable Stellar Systems (HabCat, described in Paper I), all of the nearest 100 stars and 14 old open clusters. This is further augmented by a subset of the Tycho-2 catalog based on reduced proper motions, and this larger catalog should routinely provide at least three target stars within the large primary field of view of the Allen Telescope Array. The algorithm for prioritizing objects in the full target list includes scoring based on the subset category of each target (i.e., HabCat, cluster, Tycho-2, or nearest 100), its distance (if known), and its proximity to the Sun on the color-magnitude diagram.

Subject headings: extraterrestrial intelligence — solar neighborhood

On-line material: color figure

1. INTRODUCTION

In Paper I (Turnbull & Tarter 2003), we described in detail the Catalog of Nearby Habitable Stellar Systems (HabCat), which consists of 17,129 stars selected from the *Hipparcos* Catalog according to considerations of age, variability, spectral type, metallicity, and multiplicity. Subject to observational limitations and gaps in our understanding of life, this catalog contains " habstars " that may host planetary systems that are habitable to complex life-forms. The radio search for extraterrestrial technological signals currently in progress at the SETI Institute will concentrate its observing time on these stars for the remaining observations at the Arecibo Observatory and for the first few years of observations at the Allen Telescope Array (ATA, formerly the One-hectare Telescope or 1hT), currently under construction at the Hat Creek Observatory in Northern California. In this paper, we present the remainder of the assembled target list, with the expectation that other SETI projects may find it useful.

The primary reason for augmenting HabCat with additional subsets of targets is that the ATA will speed up the current rate of target searching by more than 2 orders of magnitude, observing more than 10,000 stars per year in the full 0.5–11 GHz range (Welch & Dreher 2000). Therefore, there will be opportunity to observe many more stars than the 17,129 included in HabCat. The unique construction of the ATA will permit observation of a minimum of three targets simultaneously, using each target as an " off-source " reference for the other two in order to mitigate against terrestrial radio frequency interference (RFI). Identifying three stellar targets within the primary field of view (PFOV) of the array necessitates a much bigger target list than HabCat. The expanded target list also allows (1) exploration of the possibility that dramatically different forms of advanced life may thrive in environments humans consider hostile and (2) an increase in observing efficiency by including suitable stellar clusters.

In § 2 of this paper we briefly describe the capabilities of the ATA, which motivates us to expand our target list from HabCat. Section 3 presents the " Tycho " subset of ~250,000 dwarf stars selected from the Tycho-2 Catalog of ~2.5 million stars. Section 4 describes the " Nearest 100 " list of targets, which includes the closest (known) 100 stars regardless of age, spectral type, metallicity, multiplicity or variability. Section 5 discusses a subset of old, metal-rich open clusters included in our target list to enhance observing efficiency, and § 6 presents an algorithm for prioritizing these objects in terms of their interest to SETI.

2. CAPABILITIES OF THE ALLEN TELESCOPE ARRAY

The ATA is a joint effort by the SETI Institute and the University of California, Berkeley, currently under construction at the Hat Creek Observatory located in northern California. The ATA will consist of 350 dishes, each 6.1 m in diameter, resulting in a collecting area exceeding that of a 100 m telescope. The current development and construction timeline calls for the first 32 antennas to be operational in 2004 and the full array to come online in 2007.

The unique architecture of the ATA permits simultaneous imaging of a very large primary field of view (PFOV) for traditional radio astronomy and targeted observations of up to 16 dual-polarization synthesized beams within the PFOV for SETI, as illustrated in Figure 1. Four intermediate-frequency (IF) processors provide four independently tunable frequency channels for simultaneous observation, each with a 100 MHz bandwidth. The signal from each IF processor can feed an imaging correlator, a summing network that provides four dual-polarization beams on the sky, or both. Thus, a total of 16 spatially independent beam-pairs can be synthesized (and hence up to 16 SETI targets observed) at a maximum of four different frequencies while an image of the PFOV is simultaneously being
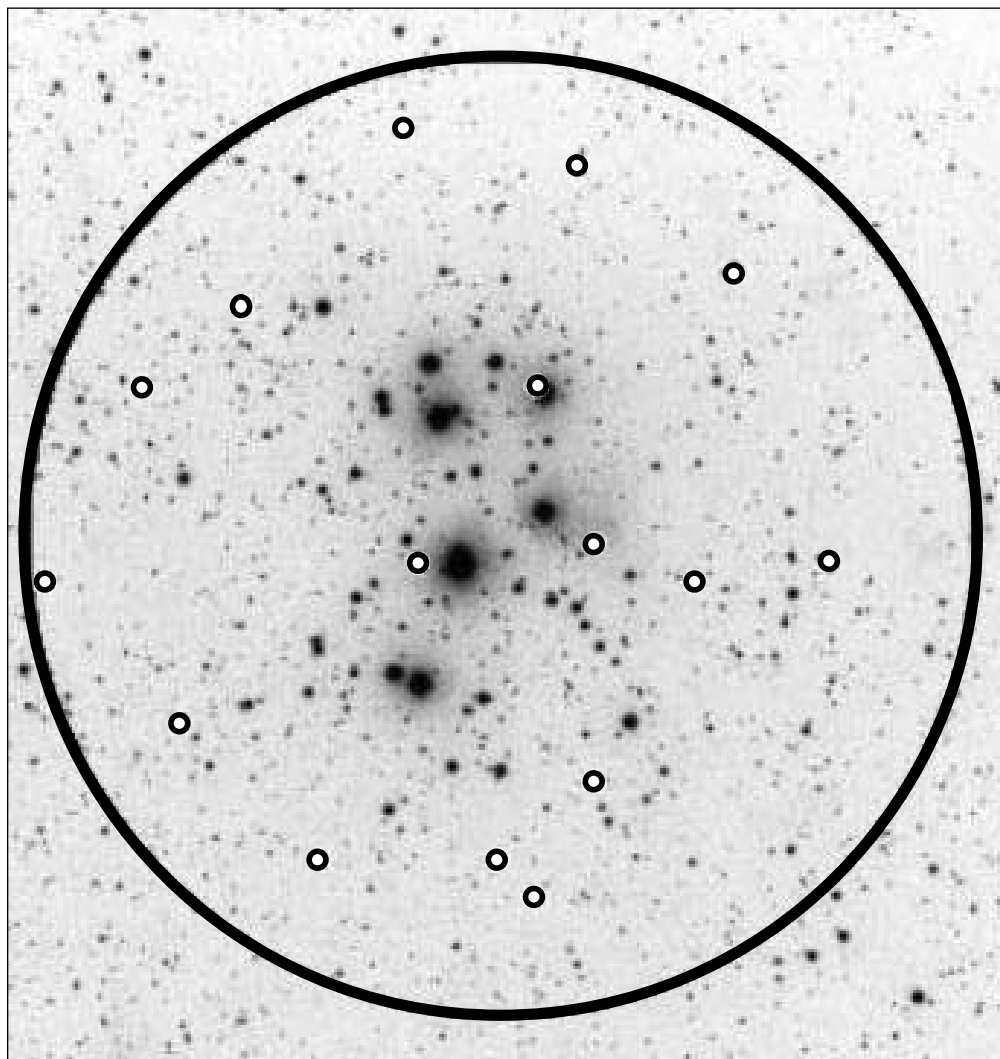
Fig. 1.—Sixteen simultaneously synthesized beam-pairs will be available to SETI and other targeted observations within the primary field of view (PFOV, 3°31 at 1 GHz) of the ATA. Each dual polarization beam (109″ at 1 GHz) can be tuned to one of four frequencies within the 0.5–11 GHz range, with a bandwidth of 100 MHz. (Image used with permission from Paul Signorelli, Las Brisas Observatory.)

generated. Finding 16 stars within every ATA PFOV would require catalogs of ∼400,000 stars (at 1 GHz) and 4 million stars (at 11 GHz) north of −34° declination.

Initially, SETI observations will have access to three dual-polarization beams. As processing becomes more affordable and larger star catalogs (e.g., from the GAIA mission) become available, observing efficiency will increase by making use of all 16 possible simultaneous SETI target and frequency combinations. The initial goal is to maintain a minimum of three spatially separated beams in operation at all times to enable an efficient filter against RFI by utilizing two of the target stars as "off-source" measurements for the third, and discarding signals detected from more than one target. While all three beams do not have to contain SETI stars for filtering of interfering signals, here we strive for three SETI targets in every PFOV.

Figure 2 illustrates how the decreasing size of the PFOV at increasing frequencies demands larger target lists for simultaneous SETI and radio astronomy observing. SETI observations will begin at the lowest frequencies where the ATA PFOV is largest. The 13,256 habstars visible from Hat Creek will permit simultaneous SETI and radio astronomy observations (i.e., there is, on average, at least one target star in any PFOV) at frequencies below ∼1.2 GHz. The solid line in Figure 2 shows the average number of HabCat stars per beam from 0.5 to 11 GHz.

For stars in the Tycho-2 catalog (which extend to much larger distances), concentration toward the Galactic plane causes the number of stars per area to be diminished at the Galactic poles by a factor of ∼2.5 from the surface density averaged over the whole sky (see Høg et al. 2000a and 2000b for an overview of Tycho-2). The dotted line in Figure 2 shows there is always more than one star (at the Galactic poles) per PFOV up to 6.8 GHz with a target list of 250,000 stars and below 2.3 GHz, there will be more than three stars per PFOV. A target list of 1 million stars (*dashed curve*) makes simultaneous SETI and radio astronomy observing possible at all frequencies and over the whole sky with the ATA, with three stars per beam at frequencies below 9 GHz. In the next section we present a large list of main-sequence stars identified in the Tycho-2 catalog, which we will use to supplement HabCat with as many reasonable SETI targets as possible.
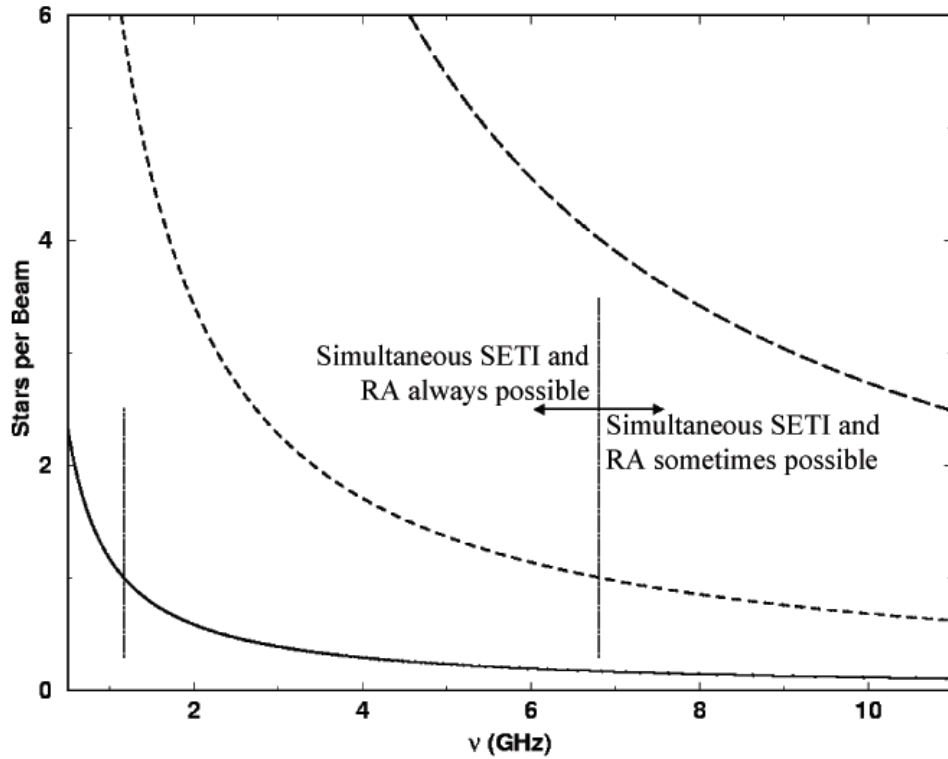
Fɪɢ. 2.—Number of stars contained in the ATA primary field of view as a function of frequency for HabCat stars (solid curve), 250,000 Tycho-2 stars (*short-dashed curve*), and 1 million stars (*long-dashed curve*). The dashed curves are for observations at the Galactic poles and thus represent the minimum number of stars per beam. The vertical lines indicate the highest frequency at which simultaneous SETI and radio astronomy observations are routinely possible.

3. THE TYCHO-2 DWARFS

The Tycho-2 Catalog of 2.5 million stars can provide targets for observation when fewer than three HabCat stars are present in the ATA PFOV. Owing to a general lack of information about the Tycho-2 stars (including age indicators, spectral types, metallicities, and multiplicity data), this list will not be as "refined" as HabCat in terms of the habitability requirements we outlined in Paper I. However, the Tycho-2 list should be comprised of late-type, main-sequence stars, to the extent that they can be separated them from the giants.

Tycho-2 lacks the parallax data necessary to determine absolute magnitudes, but the catalog contains B_T and V_T photometry and accurate proper motions (standard errors $\sim$3.5 milliarcsec yr^{-1}) for the complete sample of stars brighter than V$\sim$11. As explained in detail by Gould & Morgan (2003), the reduced proper motion (RPM) versus $B_T - V_T$ diagram can be used to separate dwarfs from giants in much the same way as a color-magnitude diagram (CMD). Here we define reduced proper motion as the quantity $H_V = V_T + 5 \log \mu - 5$, where μ is the proper motion in arcseconds per year.

3.1. *Identifying Dwarf Stars by Reduced Proper Motions*

To establish RPM criteria for excluding Tycho-2 giants, we start with the *Hipparcos* Catalog, where we have both Tycho photometry, V_T and B_T, and parallax data. Figure 3 shows the CMD in the Tycho bandpasses for *Hipparcos* stars with $B_T - V_T$ photometric uncertainties less than 0.015 mag, fractional parallax uncertainties less than 0.1, frac-

tional proper motion uncertainty less than 0.5, and no catalog flag denoting "combined photometry" in Field H48. We define in this figure the portion of the diagram that we ultimately want to keep (which is similar to that kept for HabCat). The stars in this region (displayed in black) were used to define reduced proper motion cuts in Figure 4. To remove short-lived early-type main-sequence stars, we
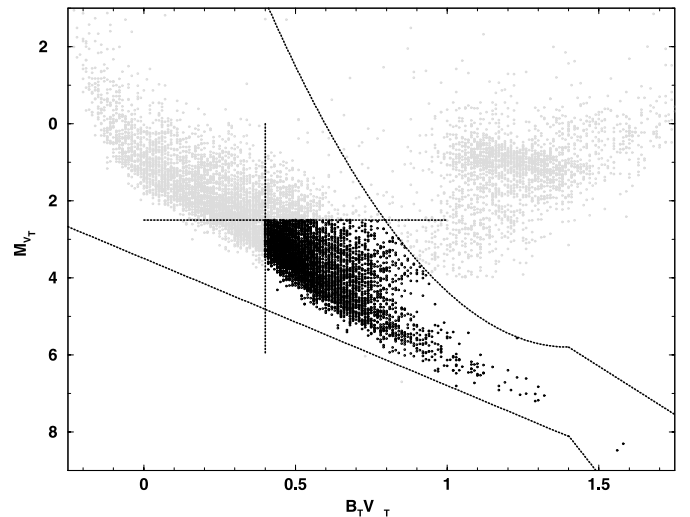

Fɪɢ. 3.—CMD for *Hipparcos* stars, in Tycho bandpasses. The desired region of the CMD is outlined and those stars (*in black*) were used to determine RPM cuts in Fig. 4.
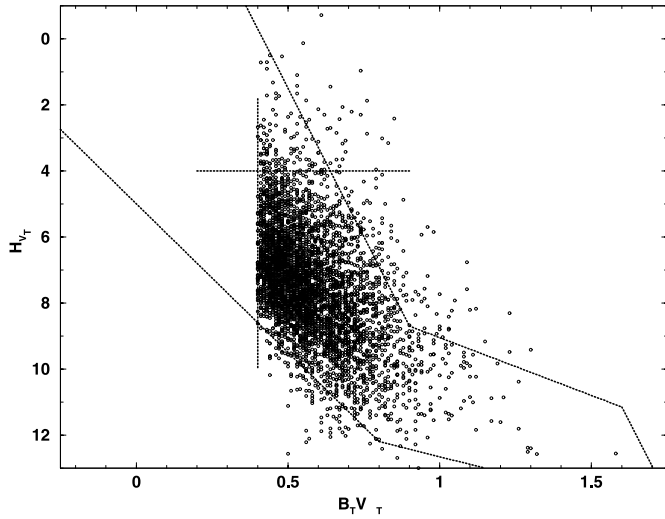
FIG. 4.—RPM diagram for *Hipparcos* stars selected according to the CMD criteria applied in Fig. 3. The solid lines indicate RPM cuts used to select Tycho-2 stars.

applied minimum $B_T - V_T$ and M_v limits, and to remove evolved stars (and extremely low-metallicity main-sequence stars), we applied cuts above and below the length of the main sequence. Thus, stars in Figure 3 *not* meeting the following criteria were removed:

$$M_V \geq 2.5 \text{ mag} ,$$

$$B_T - V_T \geq 0.4 \text{ mag} ,$$

for $0.4 < B_T - V_T \leq 1.4$ mag:

$$3.3 (B_T - V_T) + 3.5 \leq M_V \leq -9[(B_T - V_T) - 1.4]^2 + 5.8 ,$$

for $B_T - V_T \geq 1.4$ mag:

$$10(B_T - V_T) - 5.9 \leq M_V \leq 5(B_T - V_T) + 1.2 ,$$

In Figure 4, the RPM diagram for the desirable targets is shown, and cuts in RPM$-(B_T - V_T)$ space are defined to include only these stars. These are the RPM cuts used in selecting stars from the Tycho-2 catalog. Stars *not* meeting the following criteria were removed:

$$H_V \geq 4 \text{ mag} ,$$

$$B_T - V_T \geq 0.4 \text{ mag} ,$$

For $0.4 \leq B_T - V_T < 0.9$ mag: $H_V \geq 18(B_T - V_T) - 7.5 ,$

For $0.9 \leq B_T - V_T < 1.6$ mag:

$$H_V \geq 3.5(B_T - V_T) - 5.55 ,$$

For $B_T - V_T \geq 1.6$ mag: $H_V \geq 18(B_T - V_T) - 17.65 ,$

For $0.4 \leq B_T - V_T < 0.8$ mag: $H_V \leq 9(B_T - V_T) + 5 ,$

For $0.8 \leq B_T - V_T < 1.5$ mag:

$$H_V \leq 2.3(B_T - V_T) + 10.36 ,$$

For $B_T - V_T \geq 1.5$ mag: $H_V \leq 19(B_T - V_T) - 14.7 .$

Stars from the *Hipparcos* catalog satisfying these RPM cuts inhabit the color-magnitude space are shown in Figure 5a. Clearly, this is an extremely effective way of eliminating giants (which are separated from the desired sample in both $B_T - V_T$ and H_V), but bright main-sequence stars are harder to remove because they are separated from fainter dwarfs only in H_V. The fraction of stars in Figure 5 that fall *outside* the desired zone of acceptance is 11%. Nearly all of these contaminants are early-type main-sequence stars, with only 1% of RPM-selected stars falling in the post–main-sequence region. Figure 5b shows the CMD for *Hipparcos* stars that were rejected by the RPM cuts; approximately 8% of "good" main-sequence stars were falsely rejected.

The proper motion accuracies in *Hipparcos* and Tycho-2 are similar, but the *Hipparcos* sample differs from the Tycho-2 sample in that (1) distant giants were preferentially removed by the parallax uncertainty cut, and (2) the median photometric precisions

$$(\sigma_{V_T} \sim 0.006 \text{ mag}, \ \sigma_{B_T} \sim 0.006 \text{ mag})$$

are significantly better than those in the Tycho-2 sample, especially in B_T ($\sigma_{V_T} \sim 0.05$ mag, $\sigma_{B_T} \sim 0.07$ mag at $V_T = 10$–11 mag, increasing to $\sigma_{V_T} \sim 0.11$ mag, $\sigma_{B_T} \sim 0.17$ mag at $V_T = 11$–12 mag; Høg et al. 2000a). While the larger number of bright, distant giants in the Tycho-2 sample is unlikely to make a significant impact on the resulting contamination rate (those stars will primarily reside in the far upper right of the RPM diagram and be easily removed with Tycho-2 proper motion data), we must still account for the reduced photometric precision.

3.2. *Contamination Rates in an RPM Selected Sample of Stars*

To estimate the contamination and false exclusion rates we expect to have for an RPM-selected set of stars from the Tycho-2 catalog, we added artificial noise to the *B* and *V* photometry of the same set of *Hipparcos* stars used above. For each star we randomly selected a number, *x*, from a Gaussian distribution centered on zero and having a standard deviation $\sigma_x = 1$. This number was used to create a scatter term, $xN\sigma_1$, where *N* is an integer determining the magnitude of uncertainty enhancement and σ_1 is the quoted photometric standard error for the star. This scatter term (which can be positive or negative) was then added to the quoted *B* or *V* magnitude for that star, giving a new standard error $\sigma_2 = \sigma_1(N^2 + 1)^{1/2}$. The factor *N* was adjusted to give new *B* and *V* magnitudes with precisions comparable to those for stars in Tycho-2, and contamination and false exclusion rates (defining desirable and undesirable stars using the CMD for nonscattered data) were determined using the same process as above.

Table 1 shows the expected contamination and false exclusion rates for several ranges of V_T magnitude and the corresponding median standard errors in the Tycho-2 catalog. The primary effect of increasing photometric uncertainty is to scatter "good" stars *out* of the RPM-selected sample (the false exclusion rate, f_{FE}, reached 60% in the noisiest sample). The fractions of selected stars that are of early-type main-sequence (f_{EMS}, $M_V \leq 2.5$) and giant stars (f_G) increase less dramatically, reaching 21% and 12%, respectively, in the worst case. These numbers are slight overestimates, because the fainter magnitude limit of Tycho-2 endows the catalog with proportionately fewer bright stars than *Hipparcos* (both because more faint stars
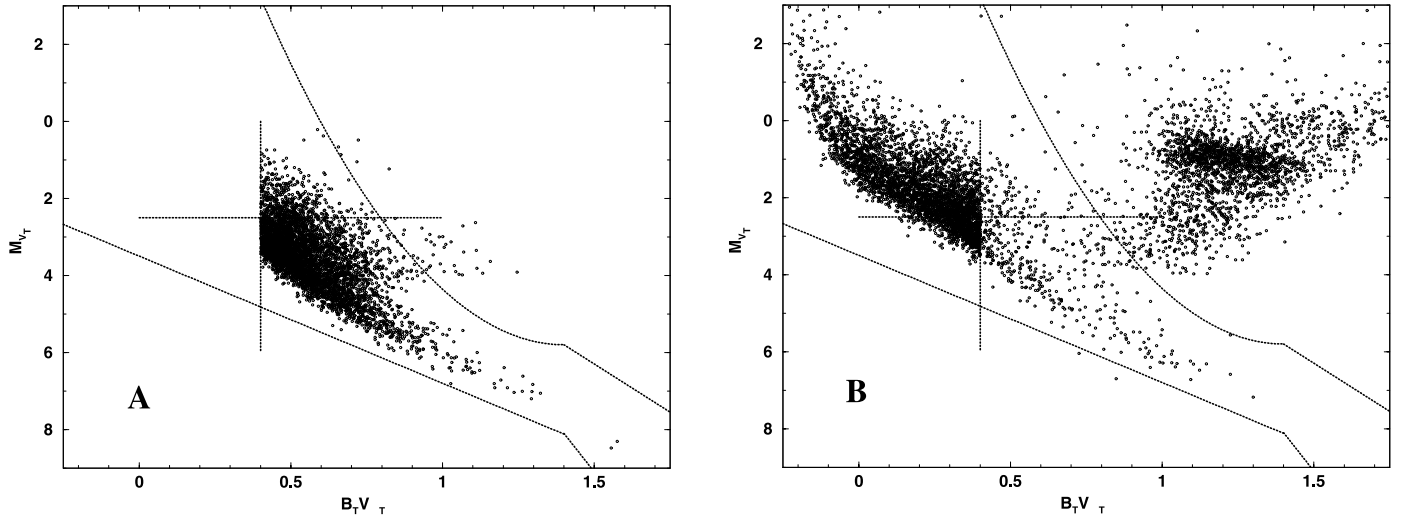
Fig. 5.—(a) Resulting CMD for *Hipparcos* stars selected according to the RPM cuts defined in Fig. 4, showing contamination of the RPM-selected sample by early-type stars and giants. Giants were easily removed, and early-type main-sequence stars are the largest source of contamination. (b) Resulting CMD for *Hipparcos* stars that were rejected by the RPM cuts, showing false rejections.

are included in the sample and because the brightest stars are seen out to distances from the Galactic plane where their space densities decrease). Thus, for Tycho-2, $\sim$48% of stars are rejected by our RPM cuts, but for the *Hipparcos* sample with similar (artificially increased) uncertainties, $\sim$58% of stars are rejected. Therefore, the true contamination and false rejection rates may be lower than the values listed in Table 1 by a factor of $\sim$0.8.

3.3. *The Tycho-2 Supplemental Target List for SETI*

We applied the derived RPM cuts to the $\sim$500,000 Tycho-2 stars with proper motion uncertainties less than 50%, no position flag (in field 2), proximity flag $\geq$999, $\sigma_{V_T} < 0.2$ mag, $\sigma_{B_T - V_T} < 0.1$ mag, and $B_T - V_T \geq 0.4$. The result is a supplemental target list of 256,610 stars with median uncertainties $\sigma_{V_T} < 0.06$ mag, $\sigma_{B_T} < 0.06$ mag, giving an expected giant star fraction of 8%–10%. When fewer than three stars from HabCat are present in the PFOV, additional targets will be selected for observation from this Tycho-2 subset. This list will allow continuous all-sky SETI observing below 7 GHz (and three targets per beam below 2.3 GHz) with the ATA. The distributions of spectral types and apparent magnitudes are shown in Figure 6. Thus, our cuts in proper motion uncertainty and $B_T - V_T$ combined with the Tycho-2 limiting magnitude for completeness have given us a list containing mostly late F-

and early G-type dwarf stars within $\sim$250 pc (assuming $M_V \sim 4$ for $B_T - V_T \sim 0.6$), a spectral distribution similar to that in HabCat (shown in Figs. 11 and 12 of Paper I) but at 3 times the average distance and with 15 times as many stars. Figure 7 shows the approximate distribution of distances assuming a transformation $M_V = 2.9 (B_T - V_T) + 2$ (a by-eye approximation to the *Hipparcos* data for RPM-selected stars), compared to the Lutz-Kelker corrected distances of all stars in HabCat. In the following sections, the SETI target list is augmented by three more subsets of stars that complement HabCat.

4. THE NEAREST 100 STARS

4.1. *SETI in the Solar Neighborhood*

The *Hipparcos* Catalog was the starting point for creating HabCat because it is the largest collection of accurate

TABLE 1
CONTAMINATION RATES FOR RPM-SELECTED STARS
IN THE TYCHO-2 CATALOG

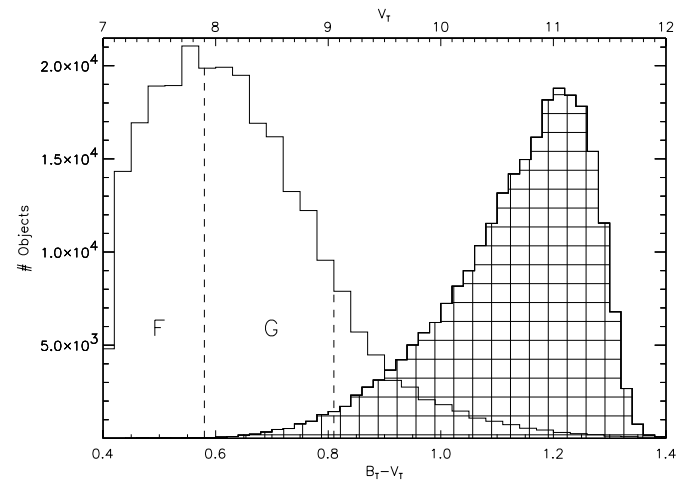| V_T	σV_T	σB_T	f_{EMS} (%)	f_G (%)	f_{FE} (%)
<7...............	0.010	0.015	9.2	3.9	9.0
7–8................	0.011	0.016	9.0	4.2	9.3
8–9................	0.014	0.020	8.9	4.7	10.2
9–10..............	0.023	0.033	10.0	5.0	13.0
10–11............	0.050	0.068	12.3	6.5	23.3
11–12............	0.114	0.173	18.1	9.5	47.0
>12...............	0.198	0.248	21.1	12.0	60.3

Fig. 6.—V_T magnitudes (*cross-hatched histogram, top axis*, 0.1 mag bins) and $B_T - V_T$ colors (*open histogram, bottom axis*, 0.03 mag bins) for Tycho-2 dwarf stars selected according to reduced proper motion data. Approximate ranges for F and G stars are shown in $B_T - V_T$.
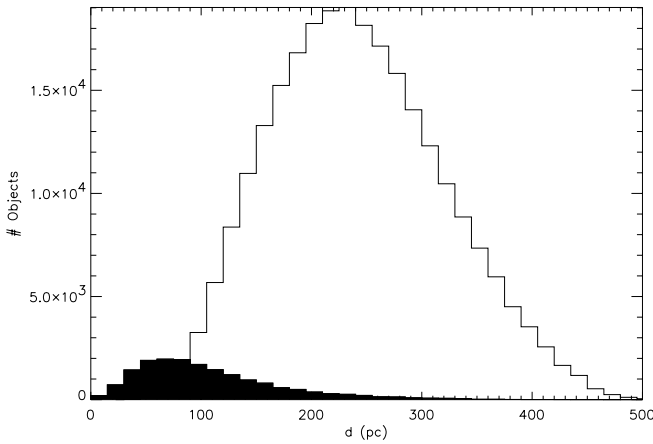
Fig. 7.—Approximate distance distribution for RPM-selected dwarfs in Tycho-2 (*open histogram*), compared to the distances of stars in HabCat (*solid histogram*), which have been corrected for the Lutz-Kelker bias.

parallax measurements in existence, and stellar distances are crucial in determining whether individual stars meet many of the habitability criteria applied in Paper I. However, the mission's magnitude limit for completeness introduced an observational bias that excluded many of the systems nearest to the Sun, a population dominated by faint M and K dwarf stars.

The "Near 100" subset, a list of the nearest 100 star systems prepared by the Research Consortium on Nearby Stars,[1] plus the third nearest system recently discovered by Teegarden et al. (2003), includes 144 total stars, of which about a third are not found in the *Hipparcos* Catalog. Table 2 lists these systems, with spectral types taken from RECONS except the "e," "sd," and "var" flags, which were taken from the Michigan Spectral Survey catalogs (Houk 1978, 1982; Houk & Cowley 1975; Houk & Smith-Moore 1988; Houk & Swift 1999). The sample includes nine white dwarfs, 27 double systems, seven multiple systems, three brown dwarf companions (GJ 845B, GL 229B, and GJ 570D), and two known planetary systems (ϵ Eri and GJ 876B). Of the 100 stars found in the *Hipparcos* Catalog, 75 were rejected from HabCat in Paper I based on habitability criteria (e.g., white dwarfs, A- and F-type stars, emission-line stars, and dynamically unfavorable multiple systems/ extrasolar planet systems). However, we have added the Near 100 objects to the SETI target list, as they provide an opportunity to explore diverse environments that could give rise to unexpected forms of complex life at distances where we are most likely to detect them.

The distance of the furthest star in the Near 100 sample, GJ 809, is $\sim$7 pc. Our sensitivity limit at that distance corresponds to a transmitter with 3.1 GW equivalent isotropic radiated power (EIRP) using the Arecibo dish and 0.7 Hz resolution after a 300 s observation (13.5 GW EIRP with the ATA with the same resolution and integration time). Such a signal is much less powerful than many terrestrial radars, but more than a thousand times stronger than commercial TV and radio broadcasts.

4.2. *The Expected Habitability of the Nearest Stars*

Seventy-five percent of the *Hipparcos* stars in the nearest 100 systems were rejected from HabCat. Table 2 indicates which objects were cut, and in the following paragraphs we briefly outline the reasons for their exclusion.

Alpha Centauri.—One system in particular, α Centauri, seems like an interesting system to SETI, both because of its proximity and because the primary of this triple system is Sunlike. However, the α Cen A and B orbit likely rules out the presence of habitable planets. Endl et al. (2001) have ruled out the presence of planets with masses greater than $\sim$2 Jupiter masses interior to 4 AU around either star (assuming orbits coplanar with the binary), but simulations by Holman & Wiegert (1999), Marzari & Scholl (2000), and Quintana et al. (2002) suggest that *terrestrial* planet formation is possible interior to $\sim$3 AU of α Cen A. The eccentricity of the binary ($e = 0.5179$; Pourbaix et al. 2002) means that over the course of one binary orbit the separation between the two stars varies from 11 AU to 36 AU, causing a nonperiodic variability in insolation at the primary's habitable zone of $\sim$3% (Hale 1996). This may not be enough to make the system uninhabitable (our insolation variability cutoff for HabCat was 3%, the variability detection limit for *Hipparcos*), but Quintana et al. (2002) also predict eccentric *planet* orbits (typically between 0.05 and 0.2 for planet orbits coplanar with the binary, up to $\sim$0.4 for planet-forming disks inclined at 45°). This would cause annual insolation variations of 20% to 125% (compared to 7% for the Earth's eccentricity of 0.016). Planets in eccentric orbits also received an increased time-averaged flux over one orbit, and thus increased global mean surface temperatures (from 15°C for Earth to 23°C for $e = 0.3$), and annual global temperature variations of 9° for $e = 0.3$, with more pronounced variations on land masses (Williams & Pollard 2002). Williams & Pollard also find that such variations probably do not rule out habitability (in terms of water loss during the hottest parts of the year), depending on the planet's inventory of volatiles, which serves to moderate climactic extremes. However, as suggested by Quintana et al. (2002), the secondary star may prevent the initial delivery of volatiles to terrestrial planets from further out in the planetary system (as envisioned by Morbidelli et al. 2000 and Robert 2001). Thus, planets in the habitable zone could be dry (which would rule out water-based life) or severely depleted in volatiles (in which case seasonal temperature variations could be much more extreme than those expected for an Earthlike planet, thereby ruling out water-based life). We maintain that the α Cen system does not belong in HabCat (and thus it will not have the priority given to HabCat objects in § 5), but it will be observed as a Near 100 object.

δ Pav and Other Near 100 G Stars.—All but one of the main-sequence G stars in the Near 100 sample were excluded from HabCat. τ Ceti and ϵ Eri were removed on the basis of low metallicity ([Fe/H] < -0.4) according to spectroscopic data from Cayrel de Strobel, Soubiran, & Ralite (2001, hereafter CSR), η Cas was detected as an unsolved variable by the *Hipparcos* mission, and ξ Boo was identified as a BY Drac type variable. The G8 IV/V star, δ Pav (HIP 99240), is SETI's most attractive target in the nearest 100 subset. This single star is metal-rich ([Fe/H] $\sim$ +0.3; CSR) and has thin disk kinematics ($U = 44$ km s^{-1}, $V = -10$ km s^{-1}, $W = -11$ km s^{-1}; Eggen 1998). It is chromospherically quiet according to the Ca II H and K activity

TABLE 2
THE NEAREST 100 LIST

No.	ID	HIP	d (pc)	Spec. Type	Name	HabCat	Note
1...............	GJ 551	70890	1.30	M5.5 Ve	Proxima Cen	No	Flare star
1...............	GJ 559 A	71683	1.34	G2 V	α Cen A	No	Binary, $a = 23.5$ AU, $e = 0.51$
1...............	GJ 559 B	71681	1.34	K0 V	α Cen B	No	Binary, $a = 23.5$ AU, $e = 0.51$
2...............	GJ 699	87937	1.83	sdM4.0 V	Barnard's Star	No	Subdwarf
3...............	SO 025300.5 +165258	...	2.4	M6.5	...	No	Teegarden et al. 2003
4...............	GJ 406	...	2.4	M6.0 V	Wolf 359	NA	...
5...............	GJ 411	54035	2.54	M2.0 V	Lalande 21185	No	Halo kinematics
6...............	GJ 244 A	32349	2.63	A1 V	Sirius	No	Var 0.06–.06 mag
6...............	GJ 244 B	...	2.63	DA2	Sirius B	NA	...
7...............	GJ 65 A	...	2.68	M5.5 V	...	NA	...
7...............	GJ 65 B	...	2.68	M6.0 V	UV Ceti	NA	...
8...............	GJ 729	92403	2.97	M3.5 Ve	Ross 154	No	Flare star
9...............	GJ 905	...	3.16	M5.5 V	Ross 248	NA	...
10...............	GJ 144	16537	3.23	K2 V	ε Eri	No	HIP microvariable, 1 planet
10...............	GJ 144 P1	...	3.23	...	...	No	$>0.92\ M_J$, 3.4AU, $e = 0.4$
11...............	GJ 887	114046	3.29	M1.5 V	Lacaille 9352	No	Halo kinematics
12...............	GJ 447	57548	3.35	M4.0 V	Ross 128	Yes	...
13...............	GJ 866 A	...	3.45	M5.0 V	EZ Aquarii	NA	...
13...............	GJ 866 B	...	3.45	...	...	NA	...
13...............	GJ 866 C	...	3.45	...	...	NA	...
14...............	GJ 280 A	37279	3.50	F5 IV–V	Procyon	No	Binary w/WD
14...............	GJ 280 B	...	3.50	DA	...	NA	...
15...............	GJ 820 A	104214	3.50	K5.0 V	61 Cygni A	No	Var > 0.6 mag
15...............	GJ 820 B	104217	3.50	K7.0 V	61 Cygni B	No	Var 0.06–0.6 mag
16...............	GJ 725 A	91768	3.53	M3.0 V	...	No	[Fe/H] < -0.4
16...............	GJ 725 B	91772	3.53	M3.5 V	...	No	[Fe/H] < -0.4
17...............	GJ 15 A	1475	3.56	M1.5 V	...	No	Var < 0.06 mag
17...............	GJ 15 B	...	3.56	M3.5 V	...	NA	...
18...............	GJ 845 A	108870	3.63	K5 Ve	ε Indi	No	Ca II H and K var
18...............	GJ 845 B	...	3.63	T2.5	...	NA	Brown dwarf, 1450 AU
19...............	GJ 1111	...	3.63	M6.5 V	DX Cancri	NA	...
20...............	GJ 71	8102	3.64	G8 Vp	τ Ceti	No	[Fe/H] < -0.4
21...............	GJ 1061	...	3.68	M5.5 V	RECONS 1	NA	...
22...............	GJ 54.1	5643	3.72	M4.5 V	YZ Ceti	No	Flare star
23...............	GJ 273	36208	3.79	M3.5 V	Luyten's Star	Yes	...
24...............	GJ 191	24186	3.92	M1.5 V	Kapteyn's Star	No	Var 0.06–0.6 mag
25...............	GJ 825	105090	3.95	M0.0 V	AX Micro	Yes	...
26...............	GJ 860 A	110893	4.03	M3.0 V	Kruger 60	No	8 AU Binary with flare star
26...............	GJ 860 B	110923	4.03	M4.0 V	...	No	Var 0.06–0.6 mag
27...............	DEN 1048−3956	...	4.03	M9.0 V	RECONS 2	NA	...
28...............	GJ 234 A	30920	4.09	M4.5 Ve	Ross 614	No	Flare star
28...............	GJ 234 B	...	4.09	...	...	NA	...
29...............	GJ 628	80824	4.24	M3.0 V	...	Yes	...
30...............	GJ 35	3829	4.31	DZ7	...	No	Evolved star
31...............	GJ 1	439	4.36	M3.0 V	...	No	Halo kinematics
32...............	GJ 473 A	...	4.39	M5.5 V	Wolf 424	NA	...
32...............	GJ 473 B	...	4.39	...	...	NA	...
33...............	GJ 83.1	...	4.45	M4.5 V	...	NA	...
34...............	LHS 288	...	4.49	M5.5 V	...	NA	...
35...............	GJ 687	86162	4.54	M3.0 Vvar	...	No	Flare star
36...............	LHS 292	...	4.54	M6.5 V	...	NA	...
37...............	GJ 674	85523	4.54	M3.0 V	...	Yes	...
38...............	GJ 1245 A	...	4.54	M5.5 V	G208-44A	NA	...
38...............	GJ 1245 B	...	4.54	M6.0 V	G208-45	NA	...
38...............	GJ 1245 C	...	4.54	...	G208-44B	NA	...
39...............	GJ 440	57367	4.62	DQ6	...	No	Evolved star
40...............	GJ 1002	...	4.69	M5.5 V	...	NA	...
41...............	GJ 876 A	113020	4.70	M3.5 V	...	No	2 planets, unstable HZ
41...............	GJ 876 A P1	...	4.70	...	...	No	$>1.89\ M_J$, 0.2AU, $e = 0.1$
41...............	GJ 876 A P2	...	4.70	...	...	No	$>0.56\ M_J$, 0.13AU, $e = 0.3$
42...............	GJ 412 A	54211	4.85	M1.0 Vvar	...	No	Flare star
42...............	GJ 412 B	...	4.85	M5.5 V	WX UMa	NA	...
43...............	GJ 380	49908	4.86	K7.0 V	...	Yes[a]	Erroneous CCDM entry
44...............	GJ 388	50583	4.89	M3.0 V	...	No	Var < 0.06 mag

TABLE 2—*Continued*

No.	ID	HIP	d (pc)	Spec. Type	Name	HabCat	Note
45..............	GJ 832	106440	4.93	M3.0 V	. . .	Yes	. . .
46..............	LP 944−020	. . .	4.97	M9.0 V	. . .	NA	. . .
47..............	GJ 682	86214	5.01	M4.5 V	. . .	Yes	. . .
48..............	GJ 166 A	19849	5.03	K1 Ve	o 2 Eri	No	Flare star
48..............	GJ 166 B	. . .	5.03	DA4	. . .	NA	. . .
48..............	GJ 166 C	. . .	5.03	M4.5 V	. . .	NA	. . .
49..............	GJ 873	112460	5.05	M3.5 Ve	EV Lac	No	Flare star
50..............	GJ 702 A	88601	5.10	K0 V	. . .	No	Variable star, 8 AU binary
50..............	GJ 702 B	88601	5.10	K5 Ve	. . .	No	Flare star
51..............	GJ 768	97649	5.13	A7 IV–V	Altair	No	Early. . .type
52..............	GJ 1116 A	. . .	5.23	M5.5 V	. . .	NA	. . .
52..............	GJ 1116 B	. . .	5.23	. . .	. . .	NA	. . .
53..............	G099-049	. . .	5.37	M3.5 V	. . .	NA	. . .
54..............	GJ 445	57544	5.38	M3.5 V	. . .	No	Halo kinematics
55..............	GJ 1005 A	1242	5.38	M4.0 V	. . .	No	HIP mult. annex X
55..............	GJ 1005 B	. . .	5.38	. . .	. . .	NA	Orbit < 2″
56..............	GJ 526	67155	5.43	M1.5 V	. . .	Yes	. . .
57..............	LHS 1723	. . .	5.47	M3.5 V	RECONS 3	NA	. . .
58..............	LP 816−060	103039	5.49	M V	. . .	Yes	. . .
59..............	GJ 169.1 A	21088	5.54	M4.0 V	Stein 2051	No	Evolved companion
59..............	GJ 169.1 B	. . .	5.54	DC5	. . .	NA	. . .
60..............	GJ 251	33226	5.57	M3.0 V	. . .	Yes	. . .
61..............	GJ 754	. . .	5.71	M4.5 V	. . .	NA	. . .
62..............	GJ 205	25878	5.71	M1.5 V	. . .	Yes	. . .
63..............	GJ 764	96100	5.76	K0 V	. . .	No	Halo kinematics
64..............	GJ 229 A	29295	5.77	M1.0 V	. . .	Yes	. . .
64..............	GJ 229 B	. . .	5.77	T6.0 V	. . .	NA	Brown dwarf
65..............	GJ 693	86990	5.82	M4.0 V	. . .	Yes	. . .
66..............	GJ 752 A	94761	5.85	M3.0 V	. . .	Yes[a]	Erroneous Houk giant
66..............	GJ 752 B	. . .	5.85	M8.0 V	van Biesbroeck 10	NA	. . .
67..............	GJ 213	26857	5.87	M4.0 V	. . .	No	Halo kinematics
68..............	GJ 300	. . .	5.89	M3.5 V	. . .	NA	. . .
69..............	GJ 570 A	73184	5.89	K5 Ve	. . .	No	Ca II H and K var
69..............	GJ 570 B	73182	5.89	M1.0 V	. . .	Yes	. . .
69..............	GJ 570 C	. . .	5.89	. . .	. . .	NA	. . .
69..............	GJ 570 D	. . .	5.89	T8.0 V	. . .	NA	Brown dwarf
70..............	GJ 908	117473	5.93	M1.0 V	. . .	No	Halo kinematics
71..............	GJ 34 A	3821	5.94	G3 V	η Cassiopeiae	No	Var < 0.06 mag
71..............	GJ 34 B	. . .	5.94	K7.0 V	. . .	NA	. . .
72..............	GJ 588	76074	5.94	M3.0 V	. . .	Yes	. . .
73..............	GJ 285	37766	5.97	M4.0 V	. . .	No	Var 0.06–0.6 mag
74..............	GJ 663 A	84405	5.97	K1 Ve	. . .	No	Flare star
74..............	GJ 663 B	. . .	5.97	K1 Ve	. . .	NA	. . .
74..............	GJ 664	84478	5.97	K5 Ve	. . .	No	Ca II H and K var
75..............	GJ 783 A	99461	6.05	K3 V	. . .	No	Halo kinematics
75..............	GJ 783 B	. . .	6.05	M4.0 V	. . .	NA	. . .
76..............	GJ 139	15510	6.06	G5 V	. . .	No	[Fe/H] < −0.4
77..............	GJ 1221	. . .	6.07	DXP9	. . .	NA	. . .
78..............	GJ 780	99240	6.11	G8 IV/V	δ Pav	Yes	Best SETI target
79..............	GJ 268 A	34603	6.14	M4.5 Ve	. . .	No	Flare star
79..............	GJ 268 B	. . .	6.14	. . .	. . .	NA	. . .
80..............	GJ 555	71253	6.14	M3.5 V	. . .	Yes	. . .
81..............	GJ 338 A	45343	6.17	M0.0 V	. . .	Yes[a]	Erroneous CCDM $N = 4$
81..............	GJ 338 B	120005	6.17	K7.0 V	. . .	Yes[a]	Erroneous CCDM $N = 4$
82..............	GJ 2130 A	86961	6.18	M2 V	. . .	No	Triple system
82..............	GJ 2130 B	86963	6.18	M2 V	. . .	No	Below main sequence
82..............	GJ 2130 C	. . .	6.18	. . .	. . .	NA	<12 AU
83..............	GJ 784	99701	6.20	M0.0 V	. . .	Yes	. . .
84..............	GJ 581	74995	6.28	M2.5 V	. . .	Yes	. . .
85..............	GJ 896 A	116132	6.34	M3.5 Ve	. . .	No	Flare star
85..............	GJ 896 B	. . .	6.34	M4.5 V	. . .	NA	. . .
86..............	GJ 661 A	84140	6.40	M3.0 V	. . .	Yes	. . .
86..............	GJ 661 B	. . .	6.40	. . .	. . .	NA	. . .
87..............	LHS 3003	. . .	6.40	M7.0 V	. . .	NA	. . .
88..............	G180-060	. . .	6.41	Dm+	. . .	NA	. . .

TABLE 2—*Continued*

No.	ID	HIP	d (pc)	Spec. Type	Name	HabCat	Note
89...............	GJ 223.2	27998	6.45	DZ9	. . .	No	Evolved star
90...............	GJ 643	82809	6.45	M3.5 V	. . .	No	5 component system
90...............	GJ 644 A	82817	6.45	M2.5 V	. . .	No	5 component system
90...............	GJ 644 B	. . .	6.45	. . .	. . .	NA	<13 AU
90...............	GJ 644 C	. . .	6.45	M7.0 V	van Biesbroeck 8	NA	1425 AU
90...............	GJ 644 D	. . .	6.45	. . .	. . .	NA	<13 AU
91...............	GJ 892	114622	6.52	K3 V	. . .	No	Flare star
92...............	GJ 1156	. . .	6.54	M5.0 V	. . .	NA	. . .
93...............	GJ 625	80459	6.59	M1.5 V	. . .	Yes	. . .
94...............	GJ 408	53767	6.66	M2.5 V	. . .	Yes	. . .
95...............	GJ 829 A	106106	6.75	M3.5 V	. . .	Yes	. . .
95...............	GJ 829 B	. . .	6.75	. . .	. . .	NA	. . .
96...............	GJ 566 A	72659	6.78	G8 Ve	ξ Boo	No	Var < 0.06 mag
96...............	GJ 566 B	. . .	6.78	K4 Ve	. . .	NA	. . .
97...............	GJ 402	53020	6.80	M4.0 V	Wolf 358	No	HIP mult. annex X
98...............	GJ 299	40141	6.84	M4.0 V	. . .	No	Post-MS
99...............	LP 771−095 A	14101	6.86	M3	RECONS 4	No	HIP mult. annex X
99...............	LP 771−095 B	. . .	6.86	. . .	. . .	NA	. . .
99...............	LP 771−096 C	. . .	6.86	. . .	. . .	NA	. . .
100..............	GJ 880	113296	6.86	M1.5 V	. . .	Yes	. . .

[a] This object was excluded based on erroneous catalog data and has been added back into HabCat.

indicator (Henry et al. 1996), was not detected as a *ROSAT* All Sky Survey X-ray point source (Guillout et al. 1999), has a small projected rotational velocity of 3.2 ± 0.2 km s^{-1} (Reiners & Schmitt 2003), and resides slightly above the main sequence. These data all suggest that the star is the Sun's age or older (see §§ 3.4 and 3.5 in Paper I for a discussion of age indicators), and Ibukiyama & Arimoto (2002) derive an age of ∼11 Gyr by isochrone fitting. Although the SIMBAD database designates this object as a '' variable star '' based on inclusion in the New Suspected Variables catalog (Kukarkin & Kholopov 1982), no recent photometry suggests variability, and *Hipparcos* photometry confirms its stability. Six years of radial velocity measurements with the Anglo-Australian Telescope showed no variations above the 3.0 m s^{-1} uncertainties, implying that there is no planet having a mass of 0.5 Jupiter masses or more within 5 AU, and no Saturn-mass planet within 2 AU (G. W. Marcy 2003, private communication). Therefore, the habitable zone of HIP 99240 is dynamically stable for terrestrial planets unless there is a giant planet outside of 5 AU with orbital eccentricity greater than 0.5 (see Table 3 of Holman & Wiegert 1999). This star ($\delta = -66°$) was observed by Project Phoenix from the Parkes Radio Observatory in April and May of 1995, and no technological signal in the frequency range 1.2–2.8 GHz stronger than the 15 Jy detection limit was detected. Such a signal would require an omnidirectional transmitted power of 65 GW, or for a 70 m directional antenna, 84 kW of power into the transmitter (P. Backus 2003, private communication); for example, NASA's Goldstone 70 m antenna and 420 kW transmitter, pointed toward Earth, would be easily detectable at the distance of δ Pav. Although it will not be visible to the ATA, δ Pav should continue to be a high-priority target for SETI programs operating in the southern hemisphere. In § 5 we discuss the top priority targets for SETI at the ATA.

Non-Solar Type Stars.—One-third (30) of the M dwarfs in the nearest 100 systems are not found in the *Hipparcos* Catalog and were therefore not included in HabCat, although seven of those stars are part of multiple systems whose primaries were included. Many of these non-*Hipparcos* (mostly M) stars, however, would have been excluded from HabCat due to flaring activity. GJ 752 A, an M3 dwarf, was excluded based on an erroneous spectral type (M2 III) given in the Houk & Swift (1999) catalog and has been reintroduced into HabCat. GJ 338 A and B have also been reintroduced, as they are part of a habitable double system, not a quadruple system as listed in the Catalog of Components of Double and Multiple Systems (CCDM) catalog. Initially, all 19 of the K dwarfs in the Near 100 sample were excluded from HabCat for reasons such as variability detected by *Hipparcos* (including the known planetary system ϵ Eri), youth indicated by Ca II H and K line activity (Noyes, Weiss, & Vaughan 1984; Henry et al. 1996; Donahue 1993), kinematics suggestive of halo membership, or dynamical instability of the habitable zone in binary systems (see Paper I for a detailed description of all these criteria). However, GJ 380 (K3 V, excluded due to erroneous listing as a member of a binary system in the CCDM catalog) has been reintroduced into HabCat. The white dwarfs and main-sequence stars earlier than F5 were all excluded from HabCat based on a 3 Gyr habitability timescale for the development of complex lifeforms, as explained in Paper I. An updated list of HabCat stars (with merits as assigned in § 5) can be obtained via e-mail from M. Turnbull.

5. OLD OPEN CLUSTERS

The primary field of view (PFOV) for the ATA is very large (3°.31 at 1 GHz), and as many as 16 independent synthesized beams can be used to simultaneously observe target stars anywhere within that field. Clusters are therefore of interest to SETI because they allow us to search for signals from many stellar systems of a chosen age and metallicity in a single observation. Globular clusters have the highest concentration of stars in the Galaxy and they meet the minimum 3 Gyr age requirement for habstars, but their very low

metallicities and extremely high stellar densities (leading to photo-evaporation and gravitational disruption of planet-forming disks) make the presence of planetary systems unlikely (Armitage 2000; Davies & Sigurdsson 2001). This is borne out by the failure to detect planetary transits in observations carried out by Gilliland et al. (2000). Globular clusters have the added disadvantage that their large distances from Earth (from ~10 kpc for M4 out to ~70 kpc for M54) require more powerful ETI transmitters to produce signals that will be detectable on Earth.

On the other hand, open clusters are relatively nearby, they tend to have metal abundances closer to solar (Dias et al. 2002), and computations suggest that the stellar densities of open clusters are not prohibitive to planet formation (Scally & Clarke 2001; Bonnell et al. 2001; Smith & Bonnell 2001; de la Fuente Marcos & de la Fuente Marcos 1997). While most open clusters are far too young to be of interest to SETI, the literature does contain a subset of ~20 clusters that are older than the 3 Gyr timescale for habitability required for habstars in Paper I. These fascinating objects are found near or outside of the solar circle in the Galaxy and at larger distances from the Galactic plane than very young clusters but generally with $z < 1$ kpc (Janes & Phelps 1994; see Friel 1995 for an overview of old open cluster properties). The known old open clusters have heliocentric distances ranging from ~800 pc (Ruprecht 46; Dias et al. 2002) to ~8 kpc (Berkeley 20; MacMinn et al. 1994), ages as high as ~10 Gyr (e.g., Berkeley 17; Carraro, Girardi, & Chiosi 1999; Phelps 1997), and metallicities ranging from ~25% solar (e.g., Berkeley 20 at [Fe/H] ~ −0.61, Friel et al. 2002), to more than 6 times solar (e.g., NGC 6253 at [Fe/H] ~ +0.8; Twarog, Anthony-Twarog, & De Lee 2003). So far, two searches for transiting planets in old open clusters have been published. Mochejska et al. (2002) discovered 47 new, low-amplitude variables in NGC 6791, and Street et al. (2003) report 11 transit-like events in the field of NGC 6819 ($\tau \sim 2.5$ Gyr, [Fe/H] ~ 0.07), but these studies are still in progress.

Once the stars in a cluster become old enough to support complex lifeforms, we expect the total habitability of the cluster (in terms of number of habitable stars) to diminish with time as the more massive stars leave the main sequence. This could be mitigated if newly inhab-ited systems around low-mass stars arise at a rate similar to their loss, but de la Fuente Marcos & de la Fuente Marcos (2003) suggest that as clusters age the range of stellar masses that is potentially habitable shrinks, because massive stars leave the main sequence faster than planets orbiting lower mass stars can become habitable (e.g., through building up protective ozone atmospheres for land-based lifeforms, with a timescale dependent upon UV flux; Livio 1999). However, considering the variety of potential evolutionary paths for terrestrial planets of different masses and compositions orbiting stars of different spectral types, our foremost concerns are (1) that the clusters be old enough for the emergence of complex life and (2) that the metallicity be high enough for terrestrial planet formation.

Table 3 presents data taken from Chaboyer, Green, & Liebert (1999, NGC 6791 data), Dias et al. (2002), and Chen, Hou, & Wang (2003) for 14 open clusters that are roughly 3 Gyr or older in age and have metallicities greater than [Fe/H] ~ −0.4 (the same metallicity cutoff applied to stars in HabCat). The large angular sizes (as large as 25′ for M67) of many of these clusters can still be accommodated by the large PFOV of the ATA, even at the highest frequency now being considered for SETI observations (11 GHz). For observations with the ATA, the entire PFOV will be observed with an imaging correlator using the best spectral resolution (~1 kHz), at the same time that individual stars within the cluster are being observed with up to 16 synthesized beams using the SETI signal processors. At the lower frequencies it will also be possible to select only those antennas whose spacings are short enough to form a synthesized beam that more nearly matches the angular size of the cluster; all stars in the cluster will be searched, but at a reduced sensitivity. The smallest clusters with diameters ~3′ could be observed with the a subarray comprised of 145 antennas at λ 21 cm. One cluster (Berkeley 17, ~7′ diameter) at +31° declination will be observable to the Project Phoenix observing program at Arecibo, but it will require a mosaic of seven single-dish beams to include the entire cluster at 1 GHz. Three of the clusters in Table 3 will be unobservable with the ATA ($\delta < -40°$), but they have been included to make this list useful to observers at facilities in the Southern Hemisphere.

TABLE 3
OLD OPEN CLUSTERS

Name	R.A. (J2000)	Decl. (J2000)	d (pc)	Age (Gyr)	[Fe/H]	Z (pc)	D (arcmin)	R_g (kpc)
Ruprecht 46	08 02	−19 28	752	4.0	−0.2	77	3	8.9
M67	08 51	+11 48	908	4.0	0	565	25	9.1
NGC 6253..................	16 59	−52 43	1510	5.0	+0.36	−165	4	7.1
NGC 188	00 47	+85 15	2047	4.3	−0.1	783	14	9.6
Collinder 261	12 38	−68 22	2190	8.9	−0.16	−215	9	7.5
Berkeley 17	05 21	+30 36	2700	12.0	−0.33	172	7	11.1
NGC 6819..................	19 41	+40 11	2754	2.5	+0.07	350	9.5	8.1
Berkeley 12	04 45	+42 41	3160	4.0	+0.07	−109	4	11.5
Berkeley 70	05 26	+41 54	4170	4.0	−0.32	260	6	12.5
NGC 1193..................	03 06	+44 23	4300	7.9	−0.29	−907	3	12.2
Melotte 66..................	07 26	−47 40	4313	2.8	−0.35	−1065	14	10.1
Berkeley 39	07 47	−04 36	4780	7.9	−0.26	837	7	12.3
Berkeley 18	05 22	+45 24	5800	4.3	+0.02	507	12	14.1
NGC 6791..................	19 21	+37 46	4830	8.0	+0.4	914	10	7.8

NOTE.—Units of right ascension are hours and minutes, and units of declination are degrees and arcminutes.

The clusters in Table 3 vary substantially in terms of membership numbers, from the fairly sparse Ru 46 (the existence of which as a true cluster has been questioned, e.g., Carraro & Patat 1995) to the much more populous clusters M67, NGC 6819, and NGC 6791 (with $\sim 10^3$ members or more). Although observing more stars per observation is generally an advantage for SETI, the dynamics of the richest objects may be less favorable for habitable worlds, so this variety in cluster richness is desirable for the SETI target list.

With an average distance of ~ 3 kpc, these objects represent the most distant SETI targets. At this distance a signal comparable to the high gain Arecibo Planetary Radar (2×10^{13} W EIRP) would be just detectable to Project Phoenix at Arecibo (9×10^{13} W EIRP with the ATA), if that signal were aimed at Earth. An omnidirectional beacon would require 10^7 times more power to be detectable. The proximity of these clusters to the Galactic plane, however, means that at 1 GHz we expect to capture $\sim 10^7$ foreground stars in each observation.

6. PRIORITIZATION OF SETI TARGETS

In the previous sections and Paper I, we have assembled a total of $\sim 274{,}000$ targets for SETI, including the Catalog of Nearby Habitable Stellar Systems (HabCat), the Near 100, Old Open Clusters, and Tycho-2 dwarfs. In this section we present a prioritization algorithm for SETI targets, so that those targets which are the most interesting from a habitability standpoint and the nearest to Earth are observed first and most often.

6.1. *HabCat Targets and the " Top 25 " Habstars*

The most favorable targets are those included in HabCat, and the two factors we have used in determining "merit" (i.e., priority) are location on the color-magnitude diagram (CMD) and distance. The "spectral" merit is a two-dimensional Gaussian in $B-V$ and M_v, which peaks at the Sun's location on the CMD (corresponding to a merit of 1.0). The distance merit falls off as the inverse-square of distance, according to the detectability of a given transmitter power. Distance merit was chosen to dominate HabCat merits out to the distance of 50 light years (~ 15 pc, a sphere encompassing 215 habstars), where responses to the first terrestrial signals of ~ 100 years ago could be reaching us now (e.g., Marconi's transatlantic communications with the broadband Poldhu spark transmitter in 1901, which may have radiated a fraction of its power through the ionosphere at $\nu > 7$ MHz, Ratcliffe 1974). The spectral and distance merits were added together to create the spectral-distance merit:

$$M_{\mathrm{HabCat}} = M_{\mathrm{spec}} + M_{\mathrm{dist}} ,$$

where

$$M_{\mathrm{spec}} = e^{-[(M_v - 4.78)^2 / 2\sigma_{M_v}]} \times e^{-[((B-V) - 0.65)^2 / 2\sigma_{B-V}]} ,$$

$$\sigma_{M_v} = 5, \ \sigma_{B-V} = 0.25 ,$$

and

$$M_{\mathrm{dist}} = \frac{(15 \ \mathrm{pc})^2}{(\mathrm{distance, \ pc})^2} .$$

Figure 8 shows the total merit for HabCat stars as a function of distance, color-coded according to spectral merit with the
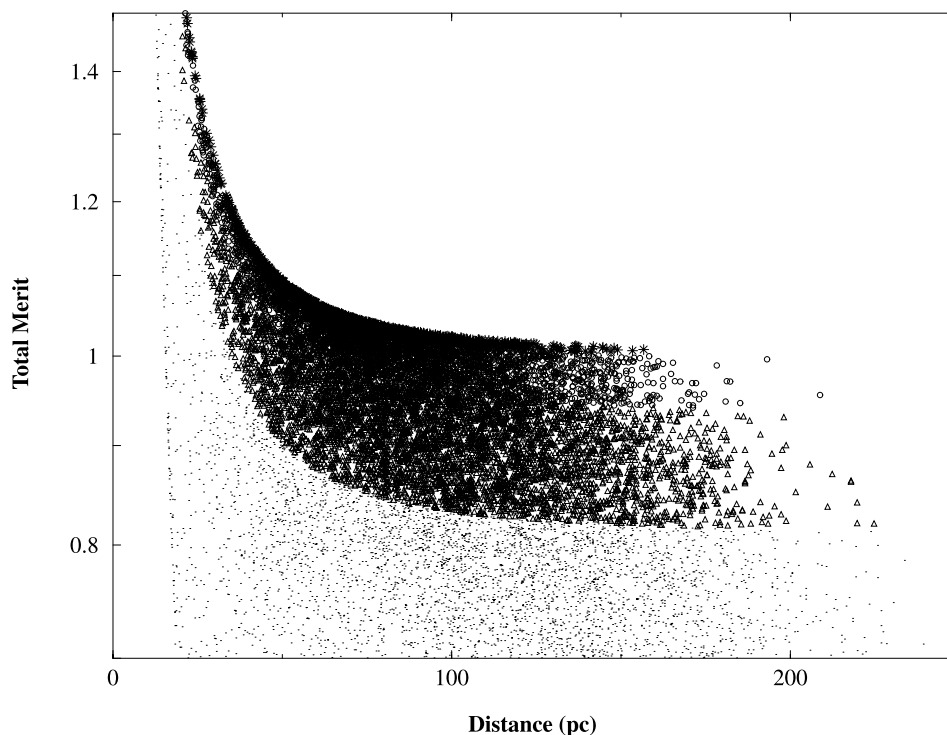

Fig. 8.—Total merit as a function of distance, color-coded by spectral merit. The 1000 most Sunlike stars are shown as stars, 1001 through 5000 as circles, 5000 through 10,000 as triangles, and 10,001 through 17,133 as dots. The total merit is dominated by distance interior to 15 pc, the response distance for Earth's first radio transmissions. [*See the electronic edition of the Journal for a color version of this figure.*]

TABLE 4
Top 25 Habstars within 25 Parsecs

HIP	R.A. (J2000)	Decl. (J2000)	Spec. Type	d (pc)	[Fe/H]	Age (Gyr)	Age Ref.	Name	Notes
61317	12 34	+41 21	G0 V	8.37	−0.21	4.05	Iso	β CVn	Solar analog, KLO
7918	01 42	+42 37	G2 V	12.64	−0.05	5.91	Iso	HD 10307	Solar analog, astrometric binary
110109	22 18	−53 38	G3 V	13.61	−0.31	3.3	Chrom	HD 211415	CCDM: 3″
79672	16 16	−08 22	G5 V	14.03	0.01	4.8	Chrom	18 Sco	CCDM: 26″, Solar Twin, KLO
113357	22 57	+20 46	G2.5 V	15.36	0.15	6.34	Iso	51 Peg	Solar analog, giant planet, KLO
27435	05 49	−04 06	G3 V	15.56	−0.24	3.19	Iso	HD 38858	KLO
100017	20 18	+66 51	G3 V	17.57	−0.21	5.55	Iso	HD 193664	Solar analog, KLO
70319	14 23	+01 15	G5 V	17.60	−0.35	5.2	Iso	HD 126053	KLO
98959	20 06	−67 19	G3 V	17.71	−0.3	7.99	Iso	HD 189567	Solar analog, AAT
34017	07 04	+29 20	G4 V	19.09	−0.16	6.68	Iso	HD 52711	Solar analog, KLO
85042	17 23	−02 23	G5 V	19.46	0.01	5.07	Iso	HD 157347	KLO
50505	10 19	+44 03	G5 V	20.64	−0.27	4.3	Chrom	HD 89269	CCDM: 144″, KLO
7339	01 35	+68 57	G6 V	20.99	0.03	5.61	Iso	HD 9407	KLO
41484	08 28	+45 39	G5 V	21.79	−0.14	6.65	Iso	HD 71148	KLO
30503	06 25	−28 47	G2 V	22.04	0.03	4.12	Iso	HD 45184	KLO
36210	07 27	−51 24	G5 V	22.51	0.05	4.7	Chrom	HD 59468	AAT
89474	18 16	+45 13	G2 V	22.69	−0.05	7.02	Iso	HD 168009	KLO
29432	06 12	+06 47	G4 V	23.12	−0.03	4	Chrom	HD 42618	KLO
9829	02 07	+24 20	G2 V	23.18	−0.23	3.1	Chrom	HD 12846	KLO
19233	04 07	−64 13	G3 V	23.19	−0.2	7.88	Iso	HD 26491	AAT
52369	10 42	−13 47	G2/3 V	23.40	−0.17	1.46	Iso	HD 92719	KLO
93185	18 59	+30 11	G0 V	23.43	−0.27	2.05	Iso	HD 176377	KLO
1499	00 19	−08 03	G5 V	23.44	0.2	5.75	Iso	HD 1461	Solar analog, KLO
33537	06 58	+22 29	G5 V	24.24	−0.33	2.3	Chrom	HD 51419	KLO
64550	13 14	−45 11	G2 V	24.47	−0.14	3.9	Chrom	HD 114853	AAT

Note.—Units of right ascension are hours and minutes, and units of declination are degrees and arcminutes.

1000 best (i.e., most Sunlike) stars shown as star symbols, 1001 through 5000 as circles, 5000 through 10,000 as triangles, and 10,001 through 17,133 as dots. The total merit values range from 0.11 (for distant, non-Sunlike stars) to 26 (for the nearest HabCat star, HIP 57548, an M4.5 V dwarf).

Looking at spectral merit alone, the 25 most interesting HabCat targets within 25 pc are listed in Table 4 (sorted by distance). The table shows an age estimate based on isochrone fitting (from Ibukiyama & Arimoto 2002) or, if this was unavailable, a "chromospheric age" calculated using Donahue's (1993) chromospheric activity-age relation and Ca II H and K line activity data from T. J. Henry & D. R. Soderblom (2002, private communication) or G. W. Marcy (2003, private communication). The isochrone ages have uncertainties of ∼0.12 dex (∼1 Gyr uncertainty at a 3 Gyr age estimate), while the chromospheric ages have larger uncertainties (0.4–0.5 dex) due to their dependence on stellar activity cycles, but stars tend to stay on the "active" or "inactive" side of $R'_{\rm HK} \sim -4.75$ (Henry et al. 1996), which corresponds to an age estimate of 2.2 Gyr. The [Fe/H] metallicities shown were taken from CSR, otherwise they were estimated from Strömgren $uvby$ photometry (Olsen 1983, 1993, 1994a, 1994b; Olsen & Perry 1984; or Eggen 1998, in the case of HIP 30503). These 25 neighbors are billions of years old, with no variability detected in *Hipparcos* photometry, and with Sunlike luminosities and temperatures. Four stars are either listed in the CCDM catalog or have "acceleration solutions" in *Hipparcos* photometry indicating probable widely separated companions, but their circumstellar habitable zones are dynamically stable according to the calculations we did in Paper I (§ 3.8.2). Twenty-three of these stars are included in the Doppler planet search project at the Keck and Lick Observatories (Butler et al. 1996;

Nidever et al. 2002; marked as "KLO" in Table 4) or at the Anglo-Australian Telescope (Tinney et al. 2001, marked "AAT"), with the other two being excluded due to nearby optical or astrometric companions. Of these 23, 51 Peg is the only star that has been found to have a giant planet companion (Mayor & Queloz 1995), but at 0.05 AU, this planet does not affect the dynamical stability of the habitable zone. The other "KLO" and "AAT" stars likely do not have any giant planet within ∼2 AU (G. W. Marcy 2003, private communication), with the exception of HIP 52369. That star was added to the planet search list in 2003 (C. McCarthy 2003, private communication), so no statement can be made about the presence or absence of planets at this time. All of the "Top 25" stars show thin disk kinematics and have metallicities greater than 40% solar (see Paper I, § 3.7). Eight of these objects are listed as solar analogs by Cayrel de Strobel & Friel (1998), including solar twin candidate 18 Sco (Porto de Mello & da Silva 1997). Twenty of these objects will be observable from the ATA. Given their distances (8–25 pc), these stars may also be prime targets for other astrobiological studies, especially the Terrestrial Planet Finder mission.

6.2. *The Near 100, Old Open Clusters, and Tycho-2 Targets*

Near 100 stars have merits determined solely by distance, and numerically they range from 0.1 (for Proxima Centauri) to 0.0003 according to

$$M_{\rm N100} = \frac{0.1 \times (1.3 \text{ pc})^2}{(\text{distance, pc})^2} .$$

The next "level" of merits were given to old open clusters (also determined by inverse-square of distance, 3×10^{-4}

to 4×10^{-6}):

$$M_{\text{cluster}} = \frac{3 \times 10^{-4} \times (752 \text{ pc})^2}{(\text{distance, pc})^2} \ .$$

Finally, the Tycho-2 stars were assigned the lowest merits, and these were based on $B_T - V_T$ color, a one-dimensional Gaussian centered on the Sun's $B_T - V_T$ color, 0.72 (converted from Cousins-Johnson $B - V = 0.65$ using Table 1 of Bessel 2000):

$$M_{\text{Tycho}} = 4 \times 10^{-6} \ e^{-[((B_T - V_T) - 0.72)^2 / 2\sigma_{B_T - V_T}]} \ ,$$

where $\sigma_{B_T - V_T} = 0.25$.

7. CONCLUDING REMARKS

HabCat has now been augmented with subsets of targets that include some non-Sunlike environments (i.e., the nearest 100 stars and stars in clusters) and improve the ATA observing efficiency (by providing one or more HabCat or Tycho-2 targets within every possible PFOV). This target list of $\sim$300,000 stars will allow us three targets per beam from 0.5 to $\sim$3 GHz, and one target per beam up to $\sim$8 GHz over the whole sky, with the situation improved somewhat close to the Galactic plane. Our most crucial need, both for improving the SETI target list and for the overall study of the biological habitability of the solar neighborhood, is measurement of the distances, metallicities, variability, masses, age indicators, and multiplicities for late F, G, and K stars in the nearest $\sim$100 pc (i.e., a complete sample down to $V \sim 14$ for stars with $0.4 < B - V < 1.0$). The detailed study of stars near the Sun has been largely neglected up to this point, but the growing field of astrobiology is creating a demand for these data, especially with regard to SETI,

NASA's Terrestrial Planet Finder mission, and ESA's Darwin mission. Survey programs with undersubscribed meter-class telescopes could potentially enlist the talents of amateur astronomers to provide intermediate-band photometry (for metallicity estimates) and monitor stellar variability for many thousands or even millions of nearby stars. Otherwise, we eagerly await the SIM and GAIA missions as contributors to this repertoire of necessary, basic data.

REFERENCES

Armitage, P. J. 2000, A&A, 362, 968
Bessell, M. S. 2000, PASP, 112, 961
Bonnell, I. A., Smith, K. W., Davies, M. B., & Horne, K. 2001, MNRAS, 322, 859
Butler, R. P., Marcy, G. W., Williams, E., McCarthy, C., Dosanjh, P., & Vogt, S. S. 1996, PASP, 108, 500
Carraro, G., Girardi, L., & Chiosi, C. 1999, MNRAS, 309, 430
Carraro, G., & Patat, F. 1995, MNRAS, 276, 563
Cayrel de Strobel, G., & Friel, E. D. 1998, in Solar Analogs: Characteristics and Optimum Candidates, ed. J. C. Hall (Flagstaff: Lowell Obs.), 93
Cayrel de Strobel, G., Soubiran, C., & Ralite, N. 2001, A&A, 373, 159 (CSR)
Chaboyer, B., Green, E. M., & Liebert, J. 1999, AJ, 117, 1360
Chen, L., Hou, J. L., & Wang, J. J. 2003, AJ, 125, 1397
Davies, M. B., & Sigurdsson, S. 2001, MNRAS, 324, 612
de La Fuente Marcos, C., & de la Fuente Marcos, R. 1997, A&A, 326, L21
———. 2003, Ap&SS, 284, 1087
Dias, W. S., Alessi, B. S., Moitinho, A., & Lépine, J. R. 2002, A&A, 389, 871
Donahue, R. A. 1993, Ph.D. thesis, New Mexico State Univ.
Eggen, O. J. 1998, AJ, 115, 2397
Endl, M., Kurster, M., Els, S., Hatzes, A. P., & Cochran, W. D. 2001, A&A, 374, 675
Friel, E. D. 1995, ARA&A, 33, 381
Friel, E. D., Janes, K. A., Tavarez, M., Scott, J., Katsants, R., Lotz, J., Hong, L., & Miller, N. 2002, AJ, 124, 2693
Gilliland, R. L., et al. 2000, ApJ, 545, L47
Gould, A., & Morgan, C. W. 2003, ApJ, 585, 1056
Guillout, P., Schmitt, J. H. M. M., Egret, D., Voges, W., Motch, C., & Sterzik, M. F. 1999, A&A, 351, 1003
Hale, A. 1996, in Circumstellar Habitable Zones: Proc. First Int. Conf., ed. L. R. Doyle (Menlo Park: Travis House Publications), 143
Henry, T. J., Soderblom, D. R., Donahue, R. A., & Baliunas, S. L. 1996, AJ, 111, 439
Høg, E., et al. 2000a, A&A, 355, L27
———. 2000b, A&A, 357, 367

Holman, M. J., & Wiegert, P. A. 1999, AJ, 117, 621
Houk, N. 1978, Catalog of Two-dimensional Spectral Types for the HD Stars, Vol. 2 (Ann Arbor: Univ. Michigan)
———. 1982, The Michigan Catalog of Two-Dimensional Spectral Types for the HD Stars, Vol. 3 (Ann Arbor: Univ. Michigan Press)
Houk, N., & Cowley, A. P. 1975, Michigan Spectral Catalog (Ann Arbor: Univ. Michigan Dep. Astron.)
Houk, N., & Smith-Moore, A. 1988, Michigan Spectral Survey, Vol. 4 (Ann Arbor: Univ. Michigan Press)
Houk, N., & Swift, C. 1999, Michigan Catalog of Two-dimensional Spectral Types for the HD Stars, Vol. 5 (Ann Arbor: Univ. Michigan Dept. Astron.)
Ibukiyama, A., & Arimoto, N. 2002, A&A, 394, 927
Janes, K. A., & Phelps, R. L. 1994, AJ, 108, 1773
Kukarkin, B. B., & Kholopov, P. N. 1982, New Catalogue of Suspected Variable Stars (Moscow: Nauka)
Livio, M. 1999, ApJ, 522, 429
MacMinn, D., Phelps, R. L., Janes, K. A., & Friel, E. D. 1994, AJ, 107, 1806
Marzari, F., & Scholl, H. 2000, ApJ, 543, 328
Mayor, M., & Queloz, D. 1995, Nature, 378, 355
Mochejska, B. J., Stanek, K. Z., Sasselov, D. D., & Szentgyorgyi, A. H. 2002, AJ, 123, 3460
Morbidelli, A., Chambers, J., Lunine, J. I., Petit, J. M., Robert, F., Valsecchi, G. B., & Cyr, K. E. 2000, Meteorics Planet. Sci., 35, 1309
Nidever, D. L., Marcy, G. W., Butler, R. P., Fischer, D. A., & Vogt, S. S. 2002, ApJ, 141, 503
Noyes, R. W., Weiss, N. O., & Vaughan, A. H. 1984, ApJ, 287, 769
Olsen, E. H. 1983, A&AS, 54, 550
———. 1993, A&AS, 102, 89
———. 1994a, A&AS, 106, 257
———. 1994b, A&AS, 104, 429
Olsen, E. H., & Perry, C. L. 1984, A&AS, 56, 229
Phelps, R. L. 1997, ApJ, 483, 826
Porto de Mello, G. F., & da Silva, L. 1997, ApJ, 482, 89
Pourbaix, D., et al. 2002, A&A, 386, 280

Quintana, E. V., Lissauer, J. J., Chambers, J. E., & Duncan, M. J. 2002, ApJ, 576, 982
Ratcliffe, J. A. 1974, Proc. IEE, 121, 1033
Reiners, A., & Schmitt, J. H. M. M. 2003, A&A, 398, 647
Robert, F. 2001, Science, 293, 105
Scally, A., & Clarke, C. 2001, MNRAS, 325, 449
Smith, K. W., & Bonnell, I. A. 2001, MNRAS, 322, L1
Street, R. A., et al. 2003, MNRAS, 340, 1287

Teegarden, B. J., et al. 2003, ApJ, 598, L51
Tinney, C. G., Butler, R. P., Marcy, G. W., Jones, H. R., Penny, A. J., Vogt, S. S., Apps, K., & Henry, G. W. 2001, ApJ, 551, 507
Turnbull, M. C., & Tarter, J. C. 2003, ApJS, 145, 181 (Paper I)
Twarog, B. A., Anthony-Twarog, B. J., & De Lee, N. 2003, AJ, 125, 1383
Welch, W. J., & Dreher, J. W. 2000, Proc. SPIE, 4015, 8
Williams, D. M., & Pollard, D. 2002, Int. J. Astrobiol., 1, 61